

Reconfiguring NASA Generic Transport Model for Normal Flight Envelope Simulation and Analysis

Ramin Norouzi

Aerospace Department, Faculty of New Sciences and Technologies
University of Tehran
Tehran, Iran
e-mail: ramin.norouzi@ut.ac.ir

Abstract—NASA Generic Transport Model (GTM) is a subscale airplane developed within the NASA Aviation Safety Program’s Integrated Resilient Aircraft Control Project with the aim of studying critical flight conditions outside the normal flight envelope without taking the risks of full-scale manned aircraft flight tests. Extensive wind tunnel tests were carried out on the model at the NASA Langley center to create extended flight envelope dataset. As part of the NASA project, a nonlinear high fidelity simulated model of GTM was developed in MATLAB® and Simulink® environment which utilizes the extensive wind tunnel test data in tabular form as the required aerodynamic database. The Simulink model is very useful in studies which require a valid high fidelity nonlinear model; however there are asymmetries in the model configuration and aerodynamic database which result in considerable amount of error if the model is used for normal flight envelope simulation and analysis. In this paper, the sources of the model asymmetry are explained and the model is reconfigured such that it can be correctly used for normal flight envelope studies. A number of simulations are provided which verify the model reconfiguration.

Keywords-generic transport model; flight envelope; model reconfiguration; simulation; Simulink; GTM-DesignSim

I. INTRODUCTION

According to the statistical report published by Boeing in August 2015, Loss of Control (LOC); within 17 accidents and a total of 1656 fatalities, is the primary contributor among different factors leading to fatal accident of commercial airliners over the years 2005-2014 [1]. Another report published by UK Civil Aviation Authority in 2013 investigating the fatal accidents of 2002-2013 shows that almost 40% of all fatal accidents were related to the loss of control, making it the major cause of the accidents [2].

A noteworthy observation in this period is that there has been a decreasing trend in the number of fatal accidents despite the increase in the number of flights, prominently due to the emerging of more accurate flight control and safety systems and more intelligent control automation systems [2]. However, still LOC holds the greatest share in fatal accidents, despite all improvements made to pilot trainings and aircraft systems.

LOC usually occurs following an upset condition which can be caused by technical failures such as control surface

defects, or external events such as icing, or internal sources such as pilot inputs, or a combination of these factors [3].

The main challenge in the prevention of LOC-led-accidents is to increase pilot’s situational awareness and develop better control systems. Previous studies have proposed various methods to assess and mitigate LOC risk, which vary from aircraft – focused methods such as designing fully protected [4], [5] and even fully automated aircraft [6] to pilot – focused methods such as improving pilot trainings via piloted simulation programs [7]. However, most of the full flight simulators used in such programs lack required extended aerodynamic database and use extrapolation on normal operating aerodynamic data when trying to simulate upset conditions, which may result in considerable errors [3].

In significant superiority over aforementioned studies, as part of NASA AvSP (Aviation safety program)’s Integrated Resilient Aircraft Control (IRAC) Project, extensive wind tunnel tests have been carried out on NASA Generic Transport Model (GTM) aircraft in the NASA Langley research center to model nonlinear regions of the extended flight envelope well beyond nominal aerodynamic data and also to construct a database for a number of structural damage cases [8], [9].

The Integrated Resilient Aircraft Control (IRAC) Project of the NASA Aviation Safety Program (AvSP) is widely researching to develop flight control laws and systems capable of recovering LOC affected aircraft, especially damaged ones, and landing them safely [9]. However, since these research control laws deal with adverse flight conditions and LOC situations, there is a great amount of risk and cost associated with flight testing them on full-scale aircraft. Therefore, as part of the Safety Program’s Integrated Resilient Aircraft Control Project, the NASA Airborne Subscale Transport Aircraft Research system (AirSTAR) was designed which provides hardware and software requirements and equipments to perform flight tests of designed control systems on a subscale model [10].

AirSTAR subscale vehicle is referred to as the Generic Transport Model (GTM), with tail number T2. It is a 5.5% twin – turbine powered, dynamically scaled aircraft which is designed with the aim of flying into drastic upset conditions and being safely recovered. Techniques [11] of dynamic scaling (i.e. full similitude using equal Froude number, ratio of the lengths for subscale to full-scale models and relative

density between subscale and full-scale models [8], [12]) were used such that the dynamics governing the subscale model are scaled accordingly so that they represent a full-scale generic transport airplane (e.g. Boeing 757) with two under wing mounted engines and a convention tail [10]. A schematic of GTM-T2 along with its control surfaces is shown in Fig 1. The tail number T2 indicates the existence of a T1 model. “The designs of both models are similar; however GTM-T2 has a lighter airframe, and so has the capability of carrying all of the required data gathering and control electronics to enable a much greater research capacity” [13]. By flying the subscale model, not only cost is considerably reduced, but more importantly, it enables flight investigation in extended regions of flight envelope that are highly risky to be tested on full-scale manned aircraft [14]. The GTM-T2 properties are shown in Table I.

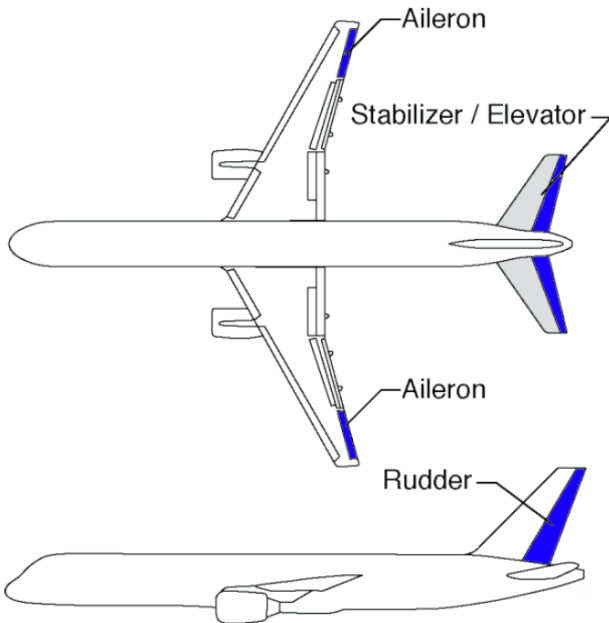


Figure 1. Schematic of 5.5% subscale GTM-T2 (based on [15]).

TABLE I. GTM-T2 PROPERTIES

Property	Quantity
Takeoff weight, W_0	257 N (26.2 kg)
Wing area, S	0.5483 m^2
Wing span, b	2.09 m
Length, l	2.59 m
Mean aerodynamic chord, \bar{c}	0.2790 m

Extensive wind tunnel tests were performed on GTM to create extended-envelope aerodynamic dataset. Test data were obtained at angles of attack as low as -5° and up to $+85^\circ$ and sideslip angles ranging from -45° to $+45^\circ$. Actually, the wind tunnel test program was initiated at NASA Langley in 2001, “using 3.5% and 5.5% subscale models representative of a modern transport configuration to study aerodynamic stability (static and dynamic), control power, configuration effects, and scale effects” [15]. Further on into the program,

the 5.5% subscale model was chosen. In fact, the reason GTM is a 5.5% scale is due to the availability of wind tunnel test data of the previous 5.5% subscale model [13].

To further mitigate the risk and cost associated with subscale flight testing, the idea of a simulated model of GTM was incorporated into AirSTAR. Hence, a high fidelity nonlinear simulation of the GTM aircraft was built from the extensive wind tunnel test data. This way; AirSTAR provides a research platform, where the research pilot is either flying the real subscale GTM aircraft or its high fidelity simulated model [8]. “The software architecture for the AirSTAR MOS (Mobile Operations Station – an integrated ground station and control room) consists of three main elements: simulation, real-time flight code, and display software.” Both the software for simulation and the flight code were primarily developed in The MathWorks MATLAB® and Simulink® environment [16], [17]. It comprises nonlinear 6 DOF equations of motion, sensors and actuators dynamics, sensors noise and bias, and telemetry uplink and downlink time delays. The dynamic model subject of our study is the GTM-T2, high fidelity, nonlinear, 6 DOF, MATLAB® – Simulink® model, also known as “GTM-DesignSim” [18]. The model’s Simulink® environment is shown in Fig. 2.

Though the “GTM-DesignSim” was initially intended for design and analysis of flight control laws, it has been found useful in many other applications where a nonlinear large-envelope flight dynamics simulation is required [18]. For instance, in [19], an adaptive controller is designed and validated using GTM – Simulink® code. In [3], a bifurcation analysis is performed to understand the flight dynamics of the open loop GTM (GTM-DesignSim model). In [20], application of retrospective cost adaptive control (RCAC) to the GTM under conditions of uncertainty and failure is investigated. In [8], an L_1 adaptive control that compensates for system uncertainty is introduced and evaluated using GTM – Simulink® software. In [21], longitudinal dynamics of GTM is incorporated through GTM-DesignSim, and a reconfigured controller design based on switching control, servomechanism, and H_2 control theory is proposed.

However, due to the original purpose of developing GTM which is studying the dynamics of airplane in regions beyond the nominal flight envelope, there are asymmetries incorporated into the GTM model within the GTM-DesignSim. These asymmetries are intended for better modeling of the aircraft behavior in upset conditions. Hence, any normal flight envelope simulation and analysis performed using the GTM-DesignSim is directly affected by these asymmetries and the results would be false. The aforementioned studies have either used the GTM-DesignSim in conditions beyond the normal flight envelope or have used the model for normal flight envelope studies but have not addressed the model asymmetries which technically makes their results inaccurate or incorrect.

In this study, the sources of the model asymmetries are elaborated and the model is reconfigured such that it can be correctly used for normal flight envelope simulations. The rest of this paper is organized as following: Section II presents the GTM-DesignSim aerodynamic database as it is

the prerequisite to understand one of the main sources of the model asymmetries, section III describes all sources of the model asymmetries, and section IV presents the model

reconfiguration along with a number of simulations intended to depict the result of this reconfiguration.

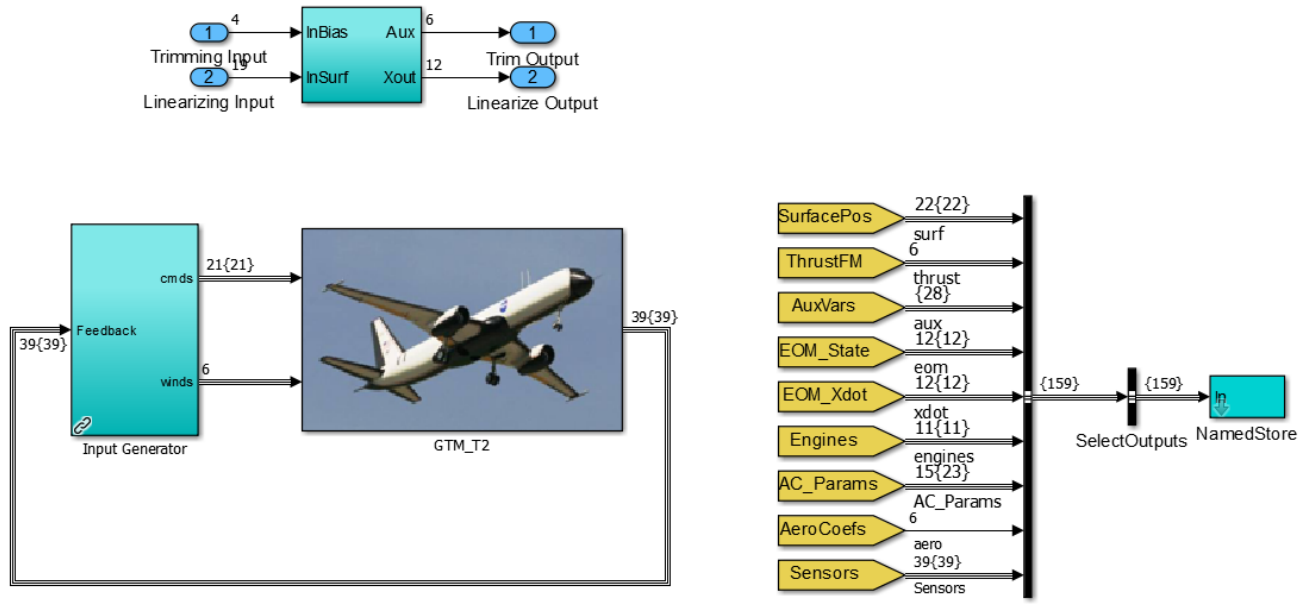


Figure 2. GTM-T2 Simulink® environment.

II. GTM-DESIGNSIM AERODYNAMIC DATABASE

The GTM Simulink® model utilizes extensive wind tunnel test data in tabular form as the required aerodynamic database. A large aerodynamic database must be handled efficiently; as it represents thousands of hours of planning and model testing. Aerodynamic data are discrete; as they are in the form of lookup table data. Meanwhile, aircraft models require data at arbitrary values of the independent variables [22]. To overcome the problem, an interpolation algorithm is used with the data. In *GTM-DesignSim*, aerodynamic data tables are linearly interpolated via the “*Interpolation Using Prelookup*” block of Simulink® “*Lookup Tables*” library.

These data tables are presented in Table II where, α and β are angles of attack and sideslip respectively, δ_r , δ_a , δ_{sp} , δ_{st} , δ_e , and δ_f , represent deflections in rudder, aileron, spoiler, stabilizer, elevator, and flap, and lgp shows landing gear position which is either up or down. \hat{p} , \hat{q} , and \hat{r} , are dimensionless angular rates equivalent to $pb/2V$, $qc/2V$, and $rb/2V$ where V is the total airspeed of the airplane and p , q and r are roll rate, pitch rate and yaw rate, respectively, and $\hat{\omega}$ is the rotation rate in rotary balance tests. Also, C_x , C_y , C_z , C_l , C_m , and C_n are forces and moments coefficients along and about X , Y , and Z axes, respectively.

As it can be seen, GTM aerodynamic data is comprised of 12 data tables with various dimensions. Each row of Table II represents one of the data tables by table dimension and

output coefficients, and can be interpreted as part of the contributions to the forces and moments coefficients. Data tables 1-8 demonstrate static contributions whilst data tables 9-12 demonstrate dynamic contributions (i.e. the ones generated by aircraft angular rates).

Data table 1 contains forces and moments coefficients for non-deflected control surfaces as a function of angles of attack and sideslip. Each one of the data tables 3-7 includes coefficients of forces and moments components from deflection of a particular control surface as a function of angles of attack and sideslip (note that data table 7 is not a function of angle of sideslip), and the deflection angle of that control surface. Data table 8 consists of forces and moments coefficients due to landing gear as a function of angle of attack and landing gear position. Data tables 9-11 are comprised of damping forces and moments derivatives which are obtained from forced oscillation tests and relate the increments in the moments or forces to the angular rates, as a function of angle of attack and the relevant dimensionless angular rate. Data table 12 represents another dynamic contribution to forces and moments coefficients arose from steady state rotation in rotary balance tests, as a function of angles of attack and sideslip and the rotation rate. The rotation rates required for dynamic contributions of data tables 9-12 (from forced oscillation and rotary balance tests) are obtained from p , q , and r using the hybrid Kalviste method [23].

TABLE II. GTM-T2 AERODYNAMIC DATA TABLES

Data Table	Table Dimensions	Output Dimensions
Aerodynamic Data Table 1	$\alpha \times \beta$	$[C_x, C_y, C_z, C_l, C_m, C_n]$
Aerodynamic Data Table 2	$\alpha \times \beta$	$[C_x, C_y, C_z, C_l, C_m, C_n]$
Aerodynamic Data Table 3	$\alpha \times \beta \times \delta_r$	$[C_x, C_y, C_z, C_l, C_m, C_n]$
Aerodynamic Data Table 4	$\alpha \times \beta \times \delta_a$	$[C_x, C_y, C_z, C_l, C_m, C_n]$
Aerodynamic Data Table 5	$\alpha \times \beta \times \delta_{sp}$	$[C_x, C_y, C_z, C_l, C_m, C_n]$
Aerodynamic Data Table 6	$\alpha \times \beta \times \delta_{st} \times \delta_e$	$[C_x, C_z, C_m]$
Aerodynamic Data Table 7	$\alpha \times \delta_f$	$[C_x, C_z, C_m]$
Aerodynamic Data Table 8	$\alpha \times \lg p$	$[C_x, C_z, C_m]$
Aerodynamic Data Table 9	$\alpha \times \hat{p}$	$[C_y, C_l, C_n]$
Aerodynamic Data Table 10	$\alpha \times \hat{q}$	$[C_y, C_l, C_n]$
Aerodynamic Data Table 11	$\alpha \times \hat{r}$	$[C_y, C_l, C_n]$
Aerodynamic Data Table 12	$\alpha \times \hat{\omega} \times \beta$	$[C_x, C_y, C_z, C_l, C_m, C_n]$

As mentioned earlier, in order to handle the discreteness of aerodynamic data, all of the 12 aerodynamic data tables are linearly interpolated inside the GTM Simulink® model. Once interpolated, three-dimensional plots can be generated from two-dimensional data tables. Such plots demonstrate variations of any of the force or moment coefficients with table dimensions. For instance, variations of axial force

coefficient C_x and yawing moment coefficient C_n with angles of attack and sideslip are shown in Fig. 3 and Fig. 4 respectively. These plots are generated from data table 1. It should be noted that for data tables with dimensions bigger than two, coefficient variations with respect to all independent variables cannot be shown in one plot, and two independent variables must be chosen for each plot.

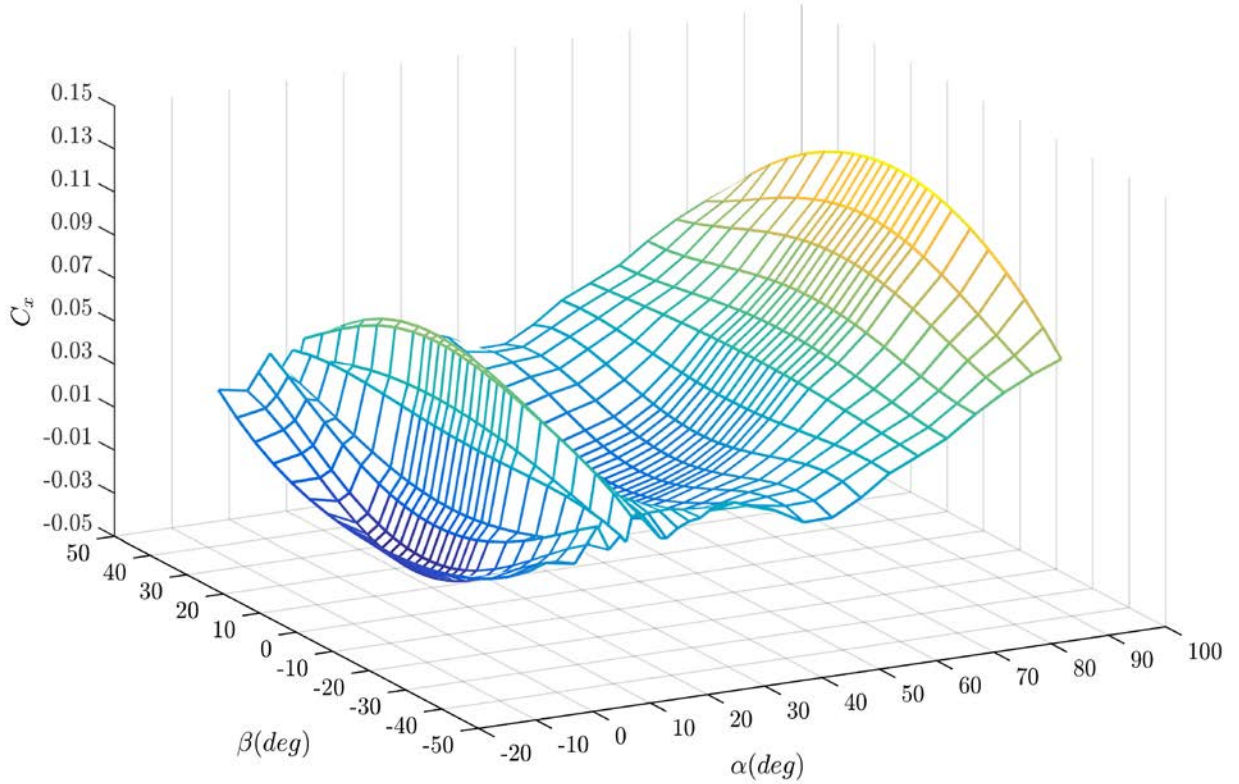


Figure 3. Variation of axial force coefficient of GTM-T2 with angle of attack and sideslip angle.

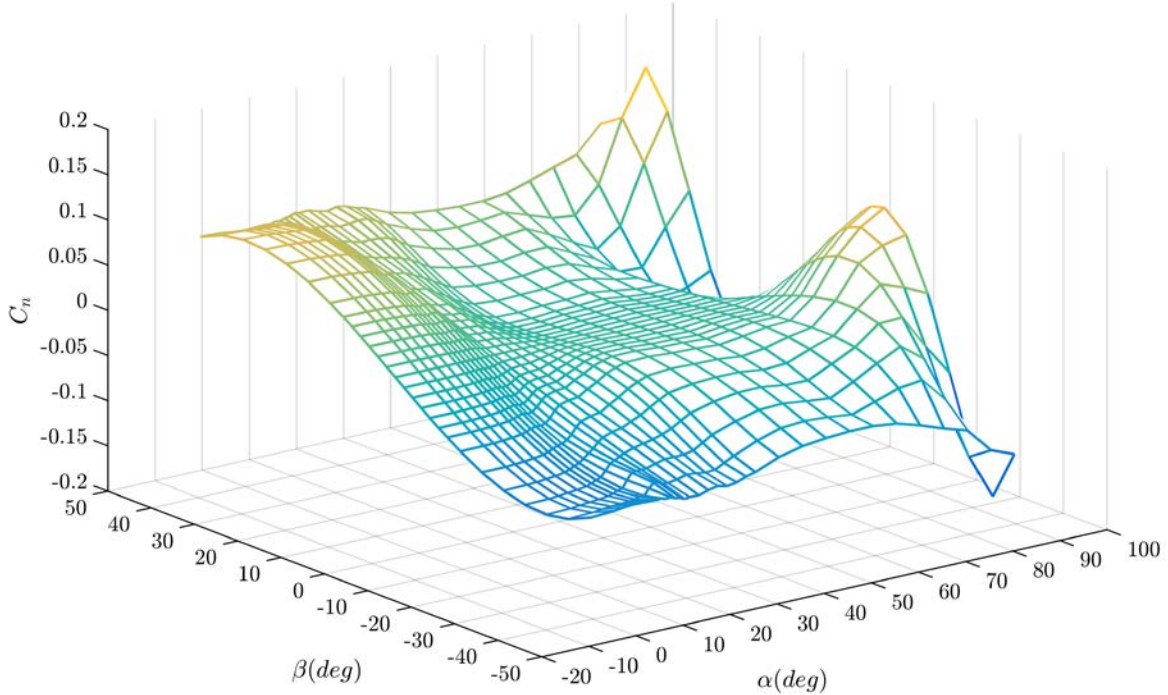


Figure 4. Variation of yawing moment coefficient of GTM-T2 with angle of attack and sideslip angle.

As can be seen in Table II, data tables 1 and 2 look similar with the same outputs and table dimensions. However, data table 2 consists of values needed to make the basic airframe aerodynamics (i.e. data of table 1) symmetric. To clarify this, first the sources of the GTM asymmetry need to be explained.

III. SOURCES OF GTM ASYMMETRY

There are 3 sources accounting for the GTM asymmetry:

- Asymmetry in the wind tunnel derived aerodynamic database
- Asymmetry in the engines mounting angles
- Offset of the CG location

Aerodynamic asymmetries (i.e. non-zero values of side force or lateral – directional moment coefficients at zero sideslip angle) in experimental data are common and it is expected that the aerodynamic asymmetry is small at low angles of attack prior to stall where the flow is not separated [15], [24]. Such asymmetries are often averaged out, as they reflect a model build error or a measurement error [24]. However, in the stall and post – stall regimes where the flow is separated, asymmetries may be large and time varying. Source of these asymmetries is not completely identified yet, though potential sources are asymmetric wing stall or asymmetric flow fields emerging from the upstream and pervading through downstream [15]. Roll instability in stall region has been investigated in [25] as a possible source of these asymmetries.

Interestingly, it was found in piloted simulations at NASA Langley that if the aircraft was perfectly symmetric, the stall behavior could seem unrealistic. A little asymmetry

and at stall the vehicle's nose will slice or a wing will drop in a manner the pilots felt was more representative [24]. Hence, it is not reasonable to average out asymmetries of wind tunnel data in both pre-stall and stall regions, as the asymmetries of stall and post-stall regions are crucial for realistic simulations. The model needs to be made symmetric just in the region prior to stall. That's where data table 2 comes from. When needed, the “*MWS.symmetric_aero_on*” flag of the model workspace is set to be 1 and corrections are applied to lateral-directional coefficients of wind tunnel database to make them symmetric. These corrections are the increments stored in data table 2 of Table II.

Since in the normal flight envelope simulations the aircraft operates in the pre-stall region and avoids stall, the symmetrized aero database are needed for such simulations.

The other two contributors to the GTM asymmetry (i.e. small difference in alignment angles between the two engines, and CG offset in the y-axis) were incorporated into the Simulink® model to match it with the measurements from the 5.5% subscale model [24]. These asymmetries also need to get corrected in order to have a perfectly symmetrical model.

IV. MODEL RECONFIGURATION

According to the previous section, there are 3 sources for the GTM asymmetry which need to get reconfigured to enable us to use the model for normal flight envelope simulations correctly.

1. Asymmetry in the aerodynamic database: as mentioned in the previous section, there is a flag named “*MWS.symmetric_aero_on*” in one of the configuration *m-files* of the *GTM-DesignSim (init_design.m)* which

- once set to 1; applies corrections from the data table 2 of the aero database and makes the aerodynamic model symmetrical.
- Asymmetry in the engines mounting angles: the difference in alignment angles between the two engines is corrected as shown in Table III :

TABLE III. ENGINES ALIGNMENT RECONFIGURATION

	Asymmetric Model			Reconfigured Model		
Left Engine Angles (deg)	0	1.98	2.22	0	1.95	1.18
Right Engine Angles (deg)	0	1.95	-1.18	0	1.95	-1.18

where the engine angles are the angular offsets of the engine with respect to X , Y , and Z axes in degree.

- Offset of the CG location: the CG offset in the y -axis is corrected as shown in Table IV :

TABLE IV. CG POSITION RECONFIGURATION

	CG Position (ft)		
Asymmetric Model	$-(LE(\bar{c}) + \bar{c} \times 0.2199)$	-0.0118	-0.9761
Reconfigured Model	$-(LE(\bar{c}) + \bar{c} \times 0.2199)$	0	-0.9761

where $LE(\bar{c})$ is the leading edge of mean aerodynamic chord.

In the following, a number of GTM maneuvers trajectories are presented which show the difference between simulations with the asymmetric model and simulations with the reconfigured model.

To create the trajectories, first the aircraft is trimmed to a steady state maneuver using the *trimgtm* function of the *GTM-DesignSim*. Then a nonlinear 6DOF simulation is run for 10 seconds initiating from that trim condition.

First in order to validate the model reconfiguration; the steady state level rectilinear flight is considered. This trim condition can be expressed as below:

$$(\dot{u}, \dot{v}, \dot{w}) = (\dot{p}, \dot{q}, \dot{r}) = (\dot{\alpha}, \dot{\beta}) = 0 \quad (1)$$

$$\dot{\phi}, \dot{\theta}, \dot{\psi}, \gamma = 0 \quad (2)$$

where, u, v, w , are airspeed components in body – fixed axes, p, q, r , are roll rate, pitch rate and yaw rate, and ϕ, θ, ψ , and γ are roll (bank) angle, pitch angle, yaw (heading) angle, and flight path angle, respectively.

It is obvious that a symmetrical aircraft should be trimmed to this steady state with undeflected lateral control surfaces, i.e. with zero degrees deflection angle of rudder and aileron. The results of trimming the asymmetric GTM and the reconfigured model to the aforementioned steady state maneuver are shown in tables V and VI:

TABLE V. ASYMMETRIC MODEL TRIM VALUES FOR LEVEL RECTILINEAR FLIGHT

Asymmetric Model			
h (ft)	10000	V (knots)	100
α (deg)	3.98	γ (deg)	0.00

β (deg)	0.00	$\dot{\phi}$ (deg/s)	0.00
p (deg/s)	0.00	$\dot{\theta}$ (deg/s)	0.00
q (deg/s)	0.00	$\dot{\psi}$ (deg/s)	0.00
r (deg/s)	0.00	δ_e (deg)	1.5026
ϕ (deg)	-0.02	δ_{th} (%)	47.13
θ (deg)	3.98	δ_a (deg)	-0.5054
ψ (deg)	0.00	δ_r (deg)	-0.0034

TABLE VI. RECONFIGURED MODEL TRIM VALUES FOR LEVEL RECTILINEAR FLIGHT

Reconfigured Model			
h (ft)	10000	V (knots)	100
α (deg)	3.99	γ (deg)	0.00
β (deg)	0.00	$\dot{\phi}$ (deg/s)	0.00
p (deg/s)	0.00	$\dot{\theta}$ (deg/s)	0.00
q (deg/s)	0.00	$\dot{\psi}$ (deg/s)	0.00
r (deg/s)	0.00	δ_e (deg)	1.5554
ϕ (deg)	0.00	δ_{th} (%)	47.30
θ (deg)	3.99	δ_a (deg)	0.00
ψ (deg)	0.00	δ_r (deg)	0.00

It can be seen that the unreconfigured model cannot be trimmed without deflecting rudder and aileron. In the other words, the asymmetric model would not follow the intended level rectilinear trajectory if rudder and aileron are not deflected. This is shown in the following figures:

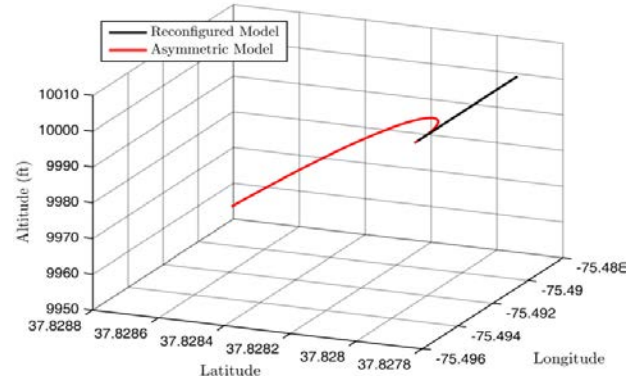


Figure 5. Comparison of models' trajectories for intended level flight with zero rudder and aileron deflections.

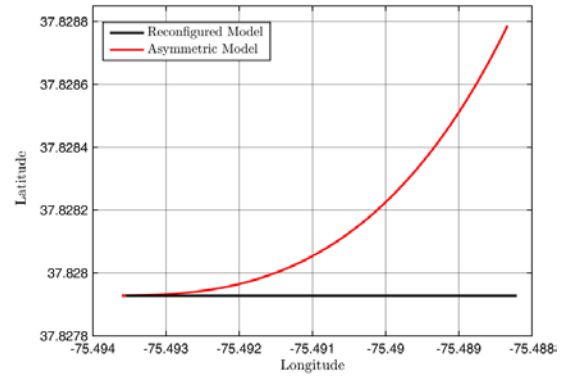


Figure 6. Top-view of models' trajectories for intended level flight with zero rudder and aileron deflection.

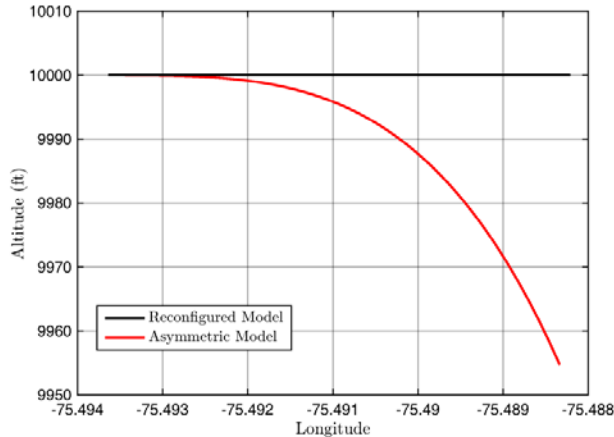


Figure 7. Side-view of models' trajectories for intended level flight with zero rudder and aileron deflection.

It can be seen in figures 5 to 7 that the reconfigured model follows the level rectilinear trajectory without any rudder or aileron deflections, as it should. However, the explained asymmetries have caused considerable error in the trajectory of the original unreconfigured *GTM-DesignSim*. The difference between the two paths is up to 50 feet in altitude and 330 feet in lateral distance over a 10s simulation.

Now that the correctness of the model reconfiguration is verified, it can be used for any normal flight envelope simulation and analysis. Figures 8 and 9 show the trajectories of the reconfigured and asymmetric models for a steady state level turn with 10 deg/s turn rate. The trim values of the reconfigured model are presented in Table VII and are considered as the initial condition of a 36s simulation.

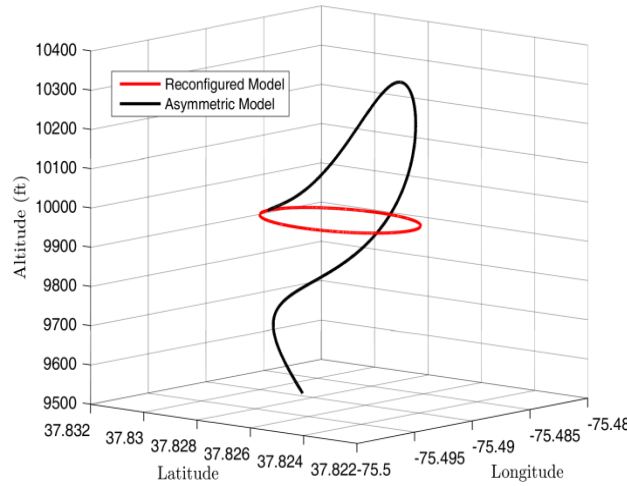


Figure 8. Comparison of models' trajectories for intended level turn.

It can be seen in Figure 8 that the reconfigured model performs a flawless circular turn without any loss of altitude. However, the trajectory obtained from the same simulation with the same initial condition shows that the original *GTM-DesignSim* performs a non steady climbing-descending maneuver if not reconfigured.

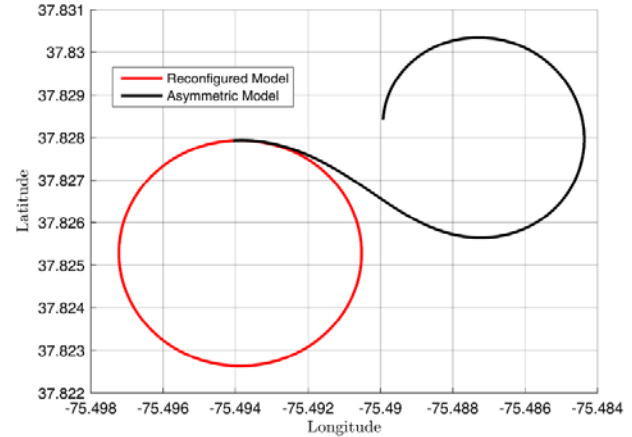


Figure 9. Top-view of models' trajectories for intended level turn.

TABLE VII. RECONFIGURED MODEL TRIM VALUES FOR LEVEL TURNING FLIGHT

Reconfigured Model			
h (ft)	V (knots)	γ (deg)	100
α (deg)	5.69	γ (deg)	0.00
β (deg)	0.00	$\dot{\phi}$ (deg/s)	0.00
p (deg/s)	-0.73	$\dot{\theta}$ (deg/s)	0.00
q (deg/s)	6.76	$\dot{\psi}$ (deg/s)	10.00
r (deg/s)	7.33	δ_e (deg)	-0.36
ϕ (deg)	42.66	δ_{th} (%)	59.35
θ (deg)	4.19	δ_a (deg)	0.24
ψ (deg)	0.00	δ_r (deg)	-0.35

V. CONCLUSION

In this paper a comprehensive review of the history of the NASA GTM, its background, and the studies applied to and utilized the model are provided. Also to address the asymmetries of the GTM Simulink® model, the technical specifications of the model's extensive aerodynamic database are described. There are three sources accounting for the asymmetries in the *GTM-DesignSim*: the aerodynamic asymmetry in the wind tunnel test data, the asymmetry in the engines mounting angles, and the offset of the CG location. These sources were originally incorporated into the model to accurately simulate the aircraft behavior in stall and post stall regions, however generate considerable error in normal regions of the flight envelope. In this paper, the model is reconfigured such that it becomes symmetrical and can be used for normal flight envelope simulations too. To verify the model reconfiguration, trajectories of the asymmetric and reconfigured models are compared in two steady state maneuvers. Results show the reconfigured model is accurate whereas the asymmetric model leads in significant error.

REFERENCES

- [1] "Statistical Summary of Commercial Jet Airplane Accidents Worldwide Operations | 1959 – 2014," Boeing Commercial Airplanes, Seattle, WA, 2015.
- [2] "Global Fatal Accident Review 2002 - 2011," TSO (The Stationery Office) on behalf of the UK Civil Aviation Authority, Norwich, UK, 2013. Available: <http://publicapps.caa.co.uk/cap1036>.

- [3] S. J. Gill, M. H. Lowenberg, S. A. Neild, B. Krauskopf, G. Puyou, and E. Coetzee, "Upset Dynamics of an Airliner Model: A Nonlinear Bifurcation Analysis," *Journal of Aircraft*, vol. 50, no. 6, Nov. 2013, pp. 1832–1842, doi: 10.2514/1.C032221.
- [4] C. Borst, F. H. Grootendorst, D. I. K. Brouwer, C. Bedoya, M. Mulder, and M. M. van Paassen, "Design and Evaluation of a Safety Augmentation System for Aircraft," *Journal of Aircraft*, vol. 51, no. 1, Jan. 2014, pp. 12–22. doi: 10.2514/1.C031500.
- [5] P. F. A. Di Donato, S. Balachandran, K. McDonough, E. Atkins, and I. Kolmanovsky, "Envelope-Aware Flight Management for Loss of Control Prevention Given Rudder Jam," *Journal of Guidance, Control, and Dynamics*, vol. 40, no. 4, Apr. 2017, pp. 1027–1041, doi: 10.2514/1.G000252.
- [6] B. Dutoi, N. Richards, N. Gandhi, D. Ward, and J. Leonard, "Hybrid Robust Control and Reinforcement Learning for Optimal Upset Recovery," *AIAA Guidance, Navigation and Control Conference and Exhibit*, 2008, doi: 10.2514/6.2008-6502.
- [7] S. Advani and J. Field, "Upset Prevention and Recovery Training in Flight Simulators," *AIAA Modeling and Simulation Technologies Conference*, 2011, doi: 10.2514/6.2011-6698.
- [8] I. Gregory, C. Cao, E. Xargay, N. Hovakimyan, and X. Zou, "L1 Adaptive Control Design for NASA AirSTAR Flight Test Vehicle," *AIAA Guidance, Navigation, and Control Conference*, 2009, doi: 10.2514/6.2009-5738.
- [9] G. Shah, "Aerodynamic Effects and Modeling of Damage to Transport Aircraft," *AIAA Atmospheric Flight Mechanics Conference and Exhibit*, 2008, doi: 10.2514/6.2008-6203.
- [10] K. Cunningham, D. Cox, D. Murri, and S. Riddick, "A Piloted Evaluation of Damage Accommodating Flight Control Using a Remotely Piloted Vehicle," *AIAA Guidance, Navigation, and Control Conference*, 2011, doi: 10.2514/6.2011-6451.
- [11] C. H. Wolowicz, J. S. Bowman, and W. P. Gilbert, "Similitude Requirements and Scaling Relationship as Applied to Model Testing," *NASA Technical Paper 1435*, August, 1979.
- [12] J. A. Ouellette, "Modeling and scaling of a flexible subscale aircraft for flight control development and testing in the presence of aeroservoelastic interactions," Ph.D. dissertation, Aerospace Eng., Virginia Polytech. Inst. State Univ., Blacksburg, VA, USA, 2013.
- [13] T. Jordan, W. Langford, and J. Hill, "Airborne Subscale Transport Aircraft Research Testbed - Aircraft Model Development," *AIAA Guidance, Navigation, and Control Conference and Exhibit*, 2005, doi: 10.2514/6.2005-6432.
- [14] T. Jordan, J. Foster, R. Bailey, and C. Belcastro, "AirSTAR: A UAV Platform for Flight Dynamics and Control System Testing," *25th AIAA Aerodynamic Measurement Technology and Ground Testing Conference*, 2006, doi: 10.2514/6.2006-3307.
- [15] J. Foster, K. Cunningham, C. Fremaux, G. Shah, E. Stewart, R. Rivers, J. Wilborn, and W. Gato, "Dynamics Modeling and Simulation of Large Transport Airplanes in Upset Conditions," *AIAA Guidance, Navigation, and Control Conference and Exhibit*, 2005, doi: 10.2514/6.2005-5933.
- [16] A. M. Murch, D. E. Cox, K. Cunningham, "Software considerations for subscale flight testing of experimental control laws" *AIAA Infotech @ Aerospace Conference and Exhibit*, 2009.
- [17] A. Murch, "A Flight Control System Architecture for the NASA AirSTAR Flight Test Infrastructure," *AIAA Guidance, Navigation and Control Conference and Exhibit*, 2008, doi: 10.2514/6.2008-6990.
- [18] "GTM_DesignSim," v1308, [Online]. Available: https://github.com/nasa/GTM_DesignSim
- [19] T.E. Gibson, A. M. Annaswamy, and S. P. Kenny, "Adaptive Control of Generic Transport Model with Modeled Failures," *Active Adaptive Controls Laboratory*, MIT, 2009.
- [20] A. Ansari and D. S. Bernstein, "Retrospective cost adaptive control of generic transport model under uncertainty and failure," *Journal of Aerospace Information Systems*, vol. 14, no. 3, Mar. 2017, pp. 123–174, doi: 10.2514/1.I010454.
- [21] B. C. Chang, H. Kwiatny, C. Belcastro, and C. Belcastro, "Aircraft Loss-of-Control Accident Prevention: Switching Control of the GTM Aircraft with Elevator Jam Failures," *AIAA Guidance, Navigation and Control Conference and Exhibit*, 2008, doi: 10.2514/6.2008-6507
- [22] B. Stevens, F. Lewis and E. Johnson, *Aircraft control and simulation*, 3rd ed. Hoboken: Wiley, 2016.
- [23] A. M. Murch, "Aerodynamic modeling of post – stall and spin dynamics of large transport airplanes," M.S. thesis, School Aerospace Eng., Georgia Inst. Tech., Atlanta, GA, USA, 2007.
- [24] D. E. Cox, private communication, January 2017.
- [25] P. Murphy, V. Klein, and N. Frink, "Unsteady Aerodynamic Modeling in Roll for the NASA Generic Transport Model," *AIAA Atmospheric Flight Mechanics Conference*, 2012, doi: 10.2514/6.2012-4652.